Processing and Application of Ceramics 12 [1] (2018) 56–65
https://doi.org/10.2298/PAC1801056F

Effect of Tris and acetic acid on the stability of titania nanoparticles in different alcohols and their electrophoretic deposition process

Morteza Farrokhi-Rad*

Department of Materials Engineering, Faculty of Engineering, Azarbaijan Shahid Madani University, P.O. Box: 53751-71379, Tabriz, Iran

Received 4 July 2017; Received in revised form 21 November 2017; Received in revised form 11 January 2018; Accepted 13 February 2018

Abstract

Tris (tris(hydroxymethyl)aminomethane) was used as the dispersant to enhance the colloidal stability of titania nanoparticles in different alcohols (methanol, ethanol, isopropanol and butanol). Acetic acid (AA) was also used to increase the ionization of Tris via acid-base reaction. The effect of Tris on the stability of suspensions in the absence as well as the presence of AA was investigated by different analysis, such as conductivity and zeta potential measurement as well as FTIR analysis. It was found that Tris is protonated and adsorbed on the titania nanoparticles. It enhances their zeta potential and thus colloidal stability. The optimum concentration of Tris increased with molecular weight of alcohol (0.1, 0.2, 0.3 and 0.6 g/l for methanolic, ethanolic, isopropanolic and butanolic suspensions, respectively). The optimum concentration of Tris decreased to 0.1 g/ l for all AA containing suspensions except the methanolic ones. Titania coating was obtained by electrophoretic deposition (EPD) performed at 60 V. The current density and in-situ kinetics of deposition were recorded during EPD. It was found that the kinetics of EPD is the fastest for the suspensions with the optimum concentration of Tris (the highest zeta potential). Calcium phosphate phases were formed on the surface of titania coating after its immersion for one week in SBF at 37.5 °C.

Keywords: *TiO_2, colloidal stability, electrophoretic deposition, Tris (tris(hydroxymethyl)aminomethane)*

I. Introduction

Titania nanostructured coatings and thin films have attracted extensive attention due to their numerous applications, such as self-cleaning [1,2], anti-bacterial [3–5], anti-fungal [6], photocatalysis [7–9], biomedical [10,11], air [12] and water [13,14] purification, etc. Various coatings methods have been used for depositing titania layer on substrates, such as sol-gel [15,16], thermal [17,18] and plasma spray [19,20], plasma electrolyte oxidation [21], physical [22] and chemical [23] vapour deposition, tape casting [24], etc. Electrophoretic deposition (EPD) is a colloidal processing technique which has been used for depositing wide range of materials onto the conductive substrates [25]. EPD is a two-step process: in the first step the charged particles dispersed in a suitable solvent move toward the oppositely charged electrode under the influence of an applied electric field (electrophoresis); in the second step they are deposited on the electrode and form a relatively dens particulate layer on it (deposition). Water electrolysis occurs at low applied electric field leading to the hydrogen and oxygen evolution at the cathode and anode, respectively. The gas evolution at the substrate electrode results in the porous deposits with inhomogeneous microstructure [26]. So, usually non-aqueous solvents (in most case alcoholic solvents) are used as the medium for EPD suspensions [27–30]. The ceramic particles acquire small surface charge in non-aqueous solvents due to their low dielectric constant. So the colloidal stability of particles is low in non-aqueous solvents due to the weak electrostatic repulsion force between them. Thus, the addition of effective dispersants into the non-aqueous suspensions is essential to prepare stable dispersions with less agglomeration. High quality coatings with fine microstructure can only be deposited from highly stable EPD suspension. In this work, the ef-

* Corresponding author: tel/fax: +98 4134327566
e-mail: *m.farrokhi.rad@azaruniv.edu, morteza_farrokhi_rad@yahoo.com*

fectiveness of Tris (tris(hydroxymethyl)aminomethane - $H_2NC(CH_2OH)_3$) as the dispersant to enhance the colloidal stability of titania nanoparticles in different alcoholic suspensions was investigated. Tris is an alkaline compound so the effect of acetic acid addition on the performance of Tris and increasing its ionization through acid-base reaction was also studied in this work.

II. Materials and methods

Tris (tris(hydroxymethyl)aminomethane) was used as the dispersant to enhance the colloidal stability of titania nanoparticles in different alcohols. Firstly, different concentrations of Tris (0, 0.1, 0.2, 0.3, 6 and 1 g/l) were dissolved in various alcohols (methanol, ethanol, isopropanol and butanol) by magnetic stirring for 30 min. To enhance the ionization of Tris via acid-base reaction, different concentrations of acetic acid (AA: 0, 0.07, 0.13, 0.2, 0.33 and 0.53 vol.%) were also added into the alcoholic solutions of Tris and magnetically stirred for 2 h. Finally, 20 g/l of titania nanoparticles (Degussa P25, primary particles size: 21±5 nm) was added to the prepared solutions and stirred for 24 h and ultrasonicated for 10 min. The conductivity of the suspensions was measured by conductivity meter (Cond 720, WTW series; Inolab). The conductivity of the alcoholic solutions of Tris without AA was also measured. FTIR analysis was used to investigate the adsorption of Tris on the titania nanoparticles. The samples for FTIR analysis were as-purchased titania P25 nanopowder as well as those extracted from different alcoholic suspensions with Tris additive (at optimum concentration). They were first centrifuged, then washed with deionized water (3 times, 6000 rpm) and finally dried at 120 °C for 24 h.

The zeta potential of the titania nanoparticles in different alcoholic suspensions with various concentrations of Tris and AA was measured by Malvern instrument. The samples for zeta potential analysis were prepared according to the method described in our previous paper [31].

Electrophoretic deposition (EPD) was performed using a two electrode cell. The two electrodes made with 316L stainless steel were placed at a distance of 1 cm and the surface area exposed to deposition was 20 mm × 20 mm. EPD was performed at 60 V (in case of methanolic suspensions EPD was performed at 20 V due to the very fast deposition rate). In-situ kinetics of deposition and current density were recorded during EPD according to the method described in our previous paper [31]. The coatings were dried at room temperature overnight. The dried coatings were sintered at 700 °C for 1 h under flowing argon gas atmosphere.

The coating deposited from the suspension with the highest zeta potential (methanolic suspension with 0.1 g/l Tris) was selected for further study. The microstructure of the coating was observed by scanning electron microscope (SEM). The bioactivity was evaluated by immersing the coating in simulated body fluid (SBF) environment at pH 7.4 and 37.5 °C for one week. SBF was prepared according to the method described by Kokubo *et al.* [32]. The ratio of the coating surface area to SBF volume was 0.1 cm^{-1}. The sample was taken out from SBF after 1 week, rinsed with deionized water and dried at room temperature for 24 h. Finally, the formation of calcium phosphate compounds on the surface of coating was investigated by SEM and EDS analysis. Electrochemical impedance spectroscopy (EIS) analysis was used to evaluate the protective properties of coating in SBF at 37.5 °C. EIS analysis was performed using a potentiostat/galvanostat Autolab 84367 and a three electrode cell (frequency range: 0.1 Hz–10 kHz). The coated and uncoated substrates, a platinum wire mesh and saturated calomel electrode (SCE) were used as the working, counter and reference electrodes, respectively.

III. Results and discussion

The electrical conductivity of different alcohols as a function of Tris content is shown in Fig. 1. As it can be seen, the conductivity of all alcohols increases with Tris concentration as a result of the following reaction:

$$\text{Tris} + \text{ROH} \longrightarrow \text{H}^+\text{Tris} + \text{RO}^- \qquad (1)$$

This reaction occurs faster in lower molecular weight alcohols due to their higher tendency to dissociation (autoprotolysis reaction) leading to increase in their conductivity with Tris addition.

Figure 2 shows the conductivity of different alcoholic suspensions of titania nanoparticles (20 g/l) with various concentrations of AA as a function of Tris content. The conductivity of all alcohols increases when 20 g/l of titania nanoparticles are added into them. Titania nanoparticles acquired positive surface charge in all 4 alcohols. The point of zero charge (PZC) is about 6 for titania. The pH of all alcohols was higher than 6 so it is expected that titania nanoparticles acquire negative surface charge in them. However, when the tita-

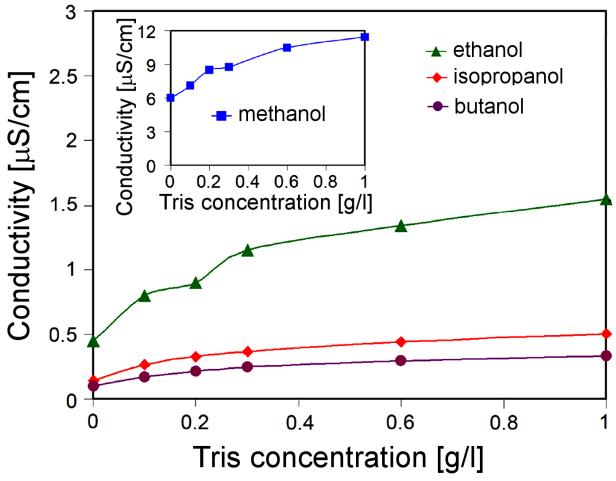

Figure 1. Flow chart for the fabrication of bismuth silicate and strontium-bismuth silicate thin films by sol-gel process

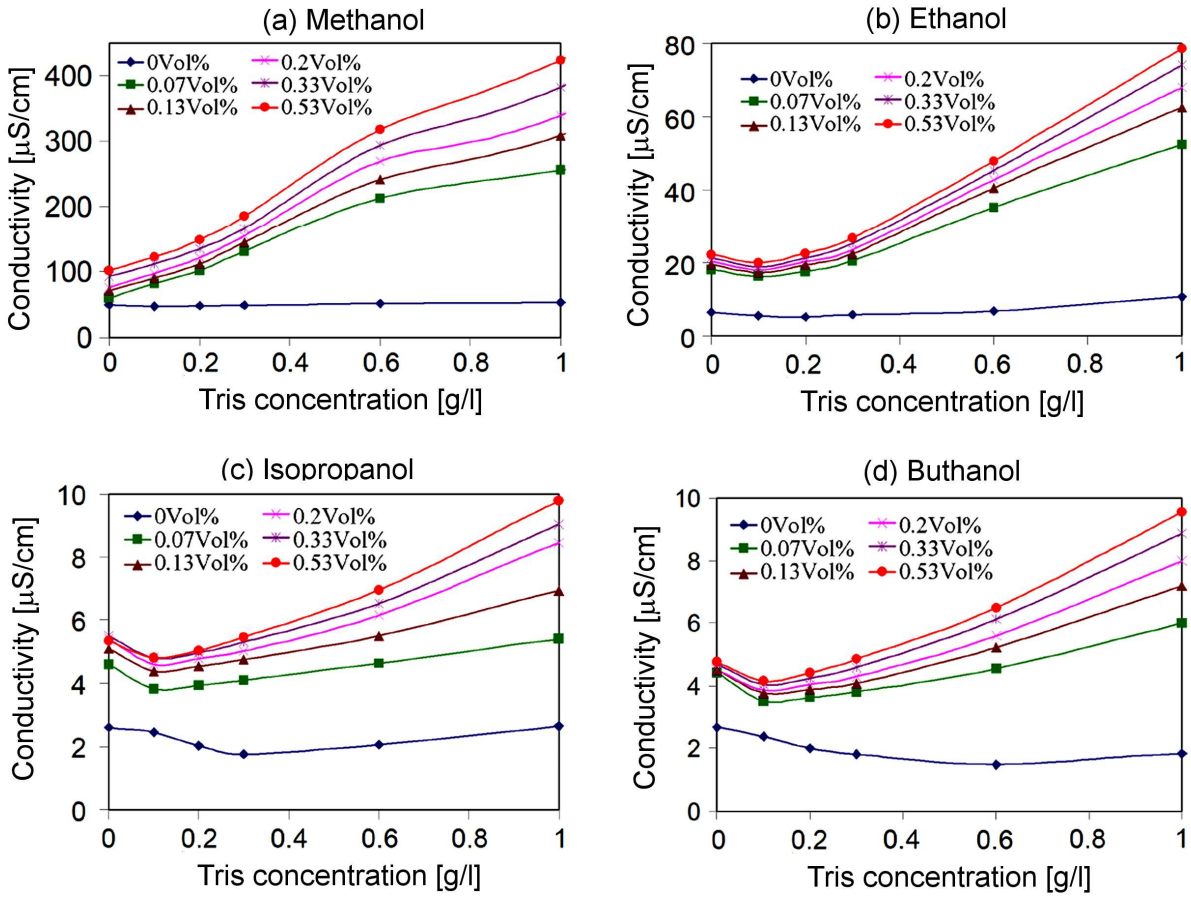

Figure 2. Electrical conductivity of different alcoholic suspensions with various concentrations of AA as a function of Tris concentration

nia nanoparticles were added into the alcohols, their pH decreased well below the PZC of titania leading to the positive surface charge for particles. Titania P25 powder have negligible amount of HCl as a process related impurity. Production process of titania P25 is based on the reaction between $TiCl_4$ and H_2 in the presence of oxygen at elevated temperatures:

$$TiCl_4 + 2\,H_2 + O_2 \longrightarrow TiO_2 + 4\,HCl \qquad (2)$$

The origin of mentioned HCl impurity is from this reaction. The presence of HCl as an impurity (< 0.3%) has also been clearly announced in the specification sheet for titania P25 by Sigma-Aldrich. The sizable drop of the pH of alcohols (2–3 units) was also observed after adding the titania P25 (20 g/l) powder into them due to the presence of HCl as the impurity in it. So the following reactions can be proposed:

$$HCl + ROH \longrightarrow Cl^- + ROH_2^+ \qquad (3)$$

$$Tris + ROH_2^+ \longrightarrow H^+Tris + ROH \qquad (4)$$

$$Tris + HCl \longrightarrow H^+Tris + Cl^- \qquad (5)$$

Reaction (3) explains pH drop as well as rise in conductivity with titania nanoparticles addition into the alcohols. The conductivity of suspensions initially decreases to a minimum value and then increases with further addition of Tris. According to reaction (4), Tris molecules take proton from ROH_2^+ ions generated through reaction (3) in the alcoholic suspensions of titania nanoparticles; reaction (5) is the net reaction showing the acid-base reaction between HCl and Tris. The H^+Tris ions generated through reaction (4), are then adsorbed on the surface of titania nanoparticles; so when Tris is added into the suspensions, the conductivity decreases to a minimum value since the mobility of free ions (ROH_2^+) is higher than that of the charged particles (H^+Tris adsorbed titania particles). The conductivity starts to increase with further addition of Tris as the surface of particles is saturated by H^+Tris ions. The conductivity has the minimum at Tris concentration of 0.1, 0.2, 0.3 and 0.6 g/l for methanolic, ethanolic, isopropanolic and butanolic suspensions, respectively. As the results of zeta potential measurement show (Fig. 3), these concentrations are the optimum concentrations of Tris in AA free suspensions. The optimum concentration of Tris is higher in larger molecular size alcohols. It can be said that the H^+Tris ions have high affinity to be adsorbed on the surface of titania nanoparticles (as the results of FTIR analysis prove the adsorption) so that the optimum concentration of Tris is mostly dependent on its protonation degree. The higher the protonation of Tris in the suspension, the lower is its optimum concentration in that suspension. Reaction (3) occurs to

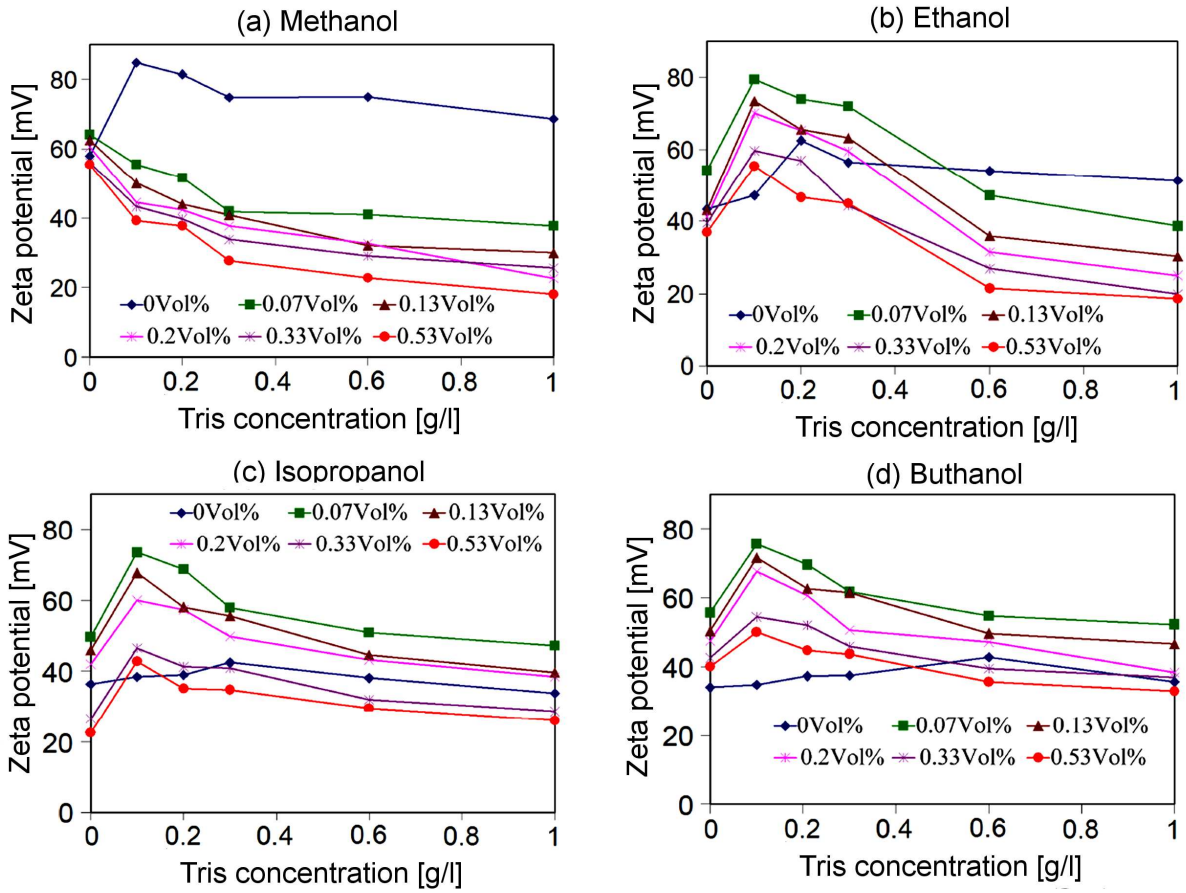

Figure 3. Zeta potential of titania nanoparticles in different alcoholic suspensions with various amounts of AA as a function of Tris concentration

higher extent in lower molecular weight alcohols; so at the same Tris content, more H^+Tris ions are generated in lower molecular weight alcohols leading to the saturation of particles surface by these ions at lower concentration of Tris. Reaction (5) occurs to more extent than reaction (1), since HCl is stronger acid than ROH; so as it can be seen in Fig. 2, after reaching the minimum value, the conductivity of suspensions increases more steeply with further addition of Tris compared to their corresponding solutions.

There is no minimum point in the conductivity curves of AA containing methanolic suspensions as a function of Tris concentration. However, the minimum point is present in the conductivity curves of other AA containing suspensions at Tris concentration of 0.1 g/l.

When Tris is added into the AA containing suspensions, the following acid-base reaction occurs between them:

$$\text{Tris} + CH_3COOH = H^+\text{Tris} + CH_3COO^- \qquad (6)$$

This reaction increases the ionic concentration of suspensions and thus their conductivity (Fig. 2). More H^+Tris ions are generated in AA containing suspensions due to the acid-base reaction between Tris and AA. So in the presence of AA, the optimum concentration of Tris is shifted to lower amounts (0.1 g/l).

The zeta potential of the titania nanoparticles in different alcoholic suspensions containing various concentrations of AA is shown against Tris amount in Fig. 3. For all alcoholic suspensions without AA, the zeta potential of the particles increases with Tris amount and reach a maximum value at its optimum concentration. However, the zeta potential decreases with further addition of Tris beyond the optimum concentration. The increase in zeta potential with Tris addition until the optimum concentration is because of the adsorption of generated H+Tris ions on the surface of titania nanoparticles leading to the rise in their surface charge and zeta potential.

The surface of particles is saturated by H^+Tris ions at its optimum concentration so that the further addition of Tris only increases the ionic strength of the suspension leading to the decrease in double layer thickness and so zeta potential [33]. The zeta potential of the particles decreases continuously as Tris is added into AA containing methanolic suspensions. As it was mentioned, the surface of the titania nanoparticles is saturated by H^+Tris ions at Tris concentration of 0.1 g/l (optimum concentration) in the methanolic suspensions without AA; so when Tris is added into methanolic suspensions with AA even at 0.1 g/l, high concentrations of H^+Tris ions are generated which is higher than that required for saturation of particles' surfaces. So the addition of Tris

into AA containing methanolic suspensions leads to the rise in their ionic strength and decrease in electrical double layer thickness and zeta potential.

In case of other AA containing alcoholic suspensions, the highest zeta potential is obtained at 0.1 g/l of Tris concentration. When Tris is added into AA containing suspensions, higher concentrations of H^+Tris ions are generated compared to those without AA so that the highest zeta potential is obtained at lower concentration of Tris. Also the value of the highest zeta potential is larger in all AA containing isopropanolic and butanolic suspensions compared to that in the similar suspensions without AA. The protonation of Tris in AA free isopropanolic and butanolic suspensions is very low so that the maximum zeta potential obtained in them is small. In the presence of AA, the protonation of Tris is promoted as a result of the acid-base reaction resulting in the subsequent increase in the value of the highest zeta potential.

Figure 4 shows the FTIR spectra of the titania nanopowder and those extracted from different alcoholic suspensions with optimum concentration of Tris. The peaks at around 1620 and 3380 cm^{-1} appeared for all samples. These peaks are attributed to O–H bonding vibration proving the water adsorption for all samples [34,35]. The spectra of powders extracted from suspensions with Tris additive have three other peaks at around 1040 cm^{-1} (C−Nstretching vibration), 2850 cm^{-1} (C−H stretching vibration) and 2930 cm^{-1} (C−H stretching vibration) proving the adsorption of Tris on the surface of titania nanoparticles [36].

The current density during EPD from alcoholic suspensions with different concentrations of AA and Tris is shown in Fig. 5. As it can be seen the current density decreases with EPD time due to the formation of ceramic layers with the higher resistivity than the suspensions deposited from them. The electrical conductivities of methanolic and ethanolic suspensions are considerably higher than that of isopropanolic and butanolic ones (Fig. 2) resulting in the higher current densities during EPD from them. At constant concentration of Tris, current density increases with AA content in the suspensions due to the increase in their conductivity.

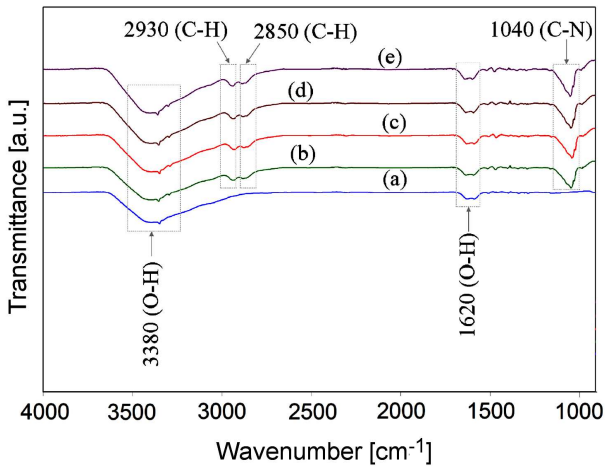

Figure 4. FTIR spectra of titania P25 nanopowder (a) and powders extracted from different alcoholic suspensions with optimum Tris concentration - methanolic with 0.1 g/l Tris (b), ethanolic with 0.2 g/l Tris (c), isopropanolic with 0.3 g/l Tris (d) and butanolic with 0.6 g/l Tris (e)

The *in-situ* kinetics of EPD from alcoholic suspensions with different concentrations of AA and Tris is shown in Fig. 6. As it can be seen in absence of AA, EPD rate is the fastest from suspensions with optimum concentration of Tris. The zeta potential and so the electrophoretic mobility of the titania nanoparticles are the highest at optimum concentration of Tris leading to the fastest kinetics of EPD for them. For AA containing methanolic suspensions, the kinetics of EPD continuously decreases with Tris addition into them due to the reduction in the zeta potential and so the mobility of particles. However, for other alcoholic suspensions with AA, EPD is the fastest from those with 0.1 g/l Tris; the kinetics of EPD decreases with further addition of Tris into these suspensions. The zeta potential and so the mobility of particles are the highest at 0.1 g/l Tris concentration in AA containing non-methanolic suspensions so that the kinetics of EPD is the fastest among them.

Also, the smaller the molecular size of the alcohol is, the faster is its EPD rate. The viscosity and the dielectric constant of alcohols increases and decreases, respectively, with their molecular size resulting in the lower mobility of particles. Thus, EPD rate is lower for the suspensions prepared from larger molecular size alcohols.

The porosity is beneficial in coatings with bioactivity and biomedical applications. Basu *et al.* [37] found that at high applied voltages (>100 V/cm) particles move so fast that they cannot find enough time to sit in the best available position to form a highly close packed microstructure. Thus, more porous coatings are deposited when EPD rate is faster. Among all alcohols used in this work, methanol has the lowest viscosity and the highest relative dielectric constant; so at the same zeta potential, the mobility of particles is the highest in methanol. Also among all methanolic suspensions, the one with 0.1 g/l Tris has the highest zeta potential (84.8 mV) and so the highest mobility resulting in the fastest EPD rate from it. So the coatings with more porous microstructures as well as less agglomeration can be deposited from this suspension. Based on these explanations, the coating deposited from the methanolic suspension with 0.1 g/l Tris was selected as the optimum one and characterized by further analysis such as SEM, bioactivity evaluation and electrochemical impedance spectroscopy. The SEM image of the coatings deposited from the methanolic suspension without and with 0.1 g/l Tris additive is shown in Fig. 7. As it can be seen the methanolic suspension with 0.1 g/l of Tris yields a coating with more even microstructure with less agglomeration. The addition of 0.1 g/l Tris into methanolic suspension leads to the considerable increase in the zeta potential of the titania

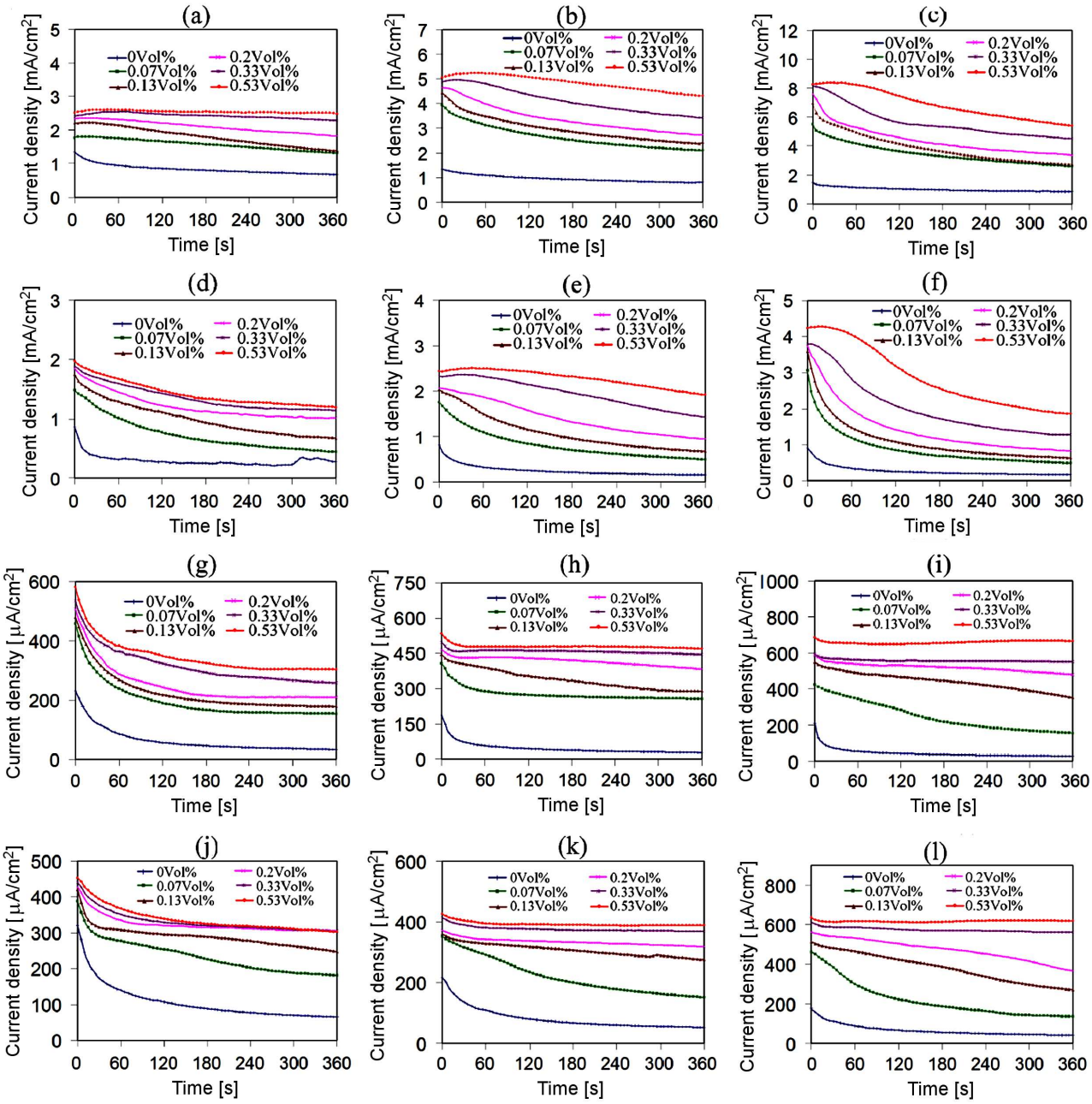

Figure 5. Current density during EPD at 60 V (for methanolic suspensions: 20 V) from different alcoholic suspensions of titania nanoparticles (20 g/l) ((a-c): methanolic, (d-f): ethanolic, (g-i): isopropanolic and (j-l): butanolic) with various concentrations of AA and Tris ((a-j): 0, (b-k): 0.3, (c-l): 0.6 g/l

nanoparticles from 58.1 to 84.8 mV. The higher the zeta potentials of particles are, the higher the electrostatic repulsive forces are between them preventing from their approaching to each other at so close distances that attractive Van der Waals forces are activated. Also it can be seen that the coating deposited from methanolic suspension without Tris has coarser pores (200–500 nm) while the one deposited from the suspension with 0.1 g/l Tris has numerous fine pores (<100 nm). There are more coarse agglomerates in the suspension without Tris so that during EPD these agglomerates move toward the substrate and deposit on it resulting in the formation of coarser pores. Thus, these coarse agglomerates are more compact with less porosity so that their accumulation on the substrate mostly results in the coarse pores. On the other hand, the agglomeration of particles is less in suspension with 0.1 g/l Tris so that the finer particles move and deposit on the substrate leading to the formation of finer pores. However, due to the higher zeta potential and so the higher mobility of the particles in suspension with 0.1 g/l Tris, they move and deposit on the substrate faster resulting in the more number of pores in the coating deposited from it. EPD coatings should be sintered at high temperatures to acquire acceptable strength and adhesion to substrate. Also the agglomerated microstructures have less sinterability so that the

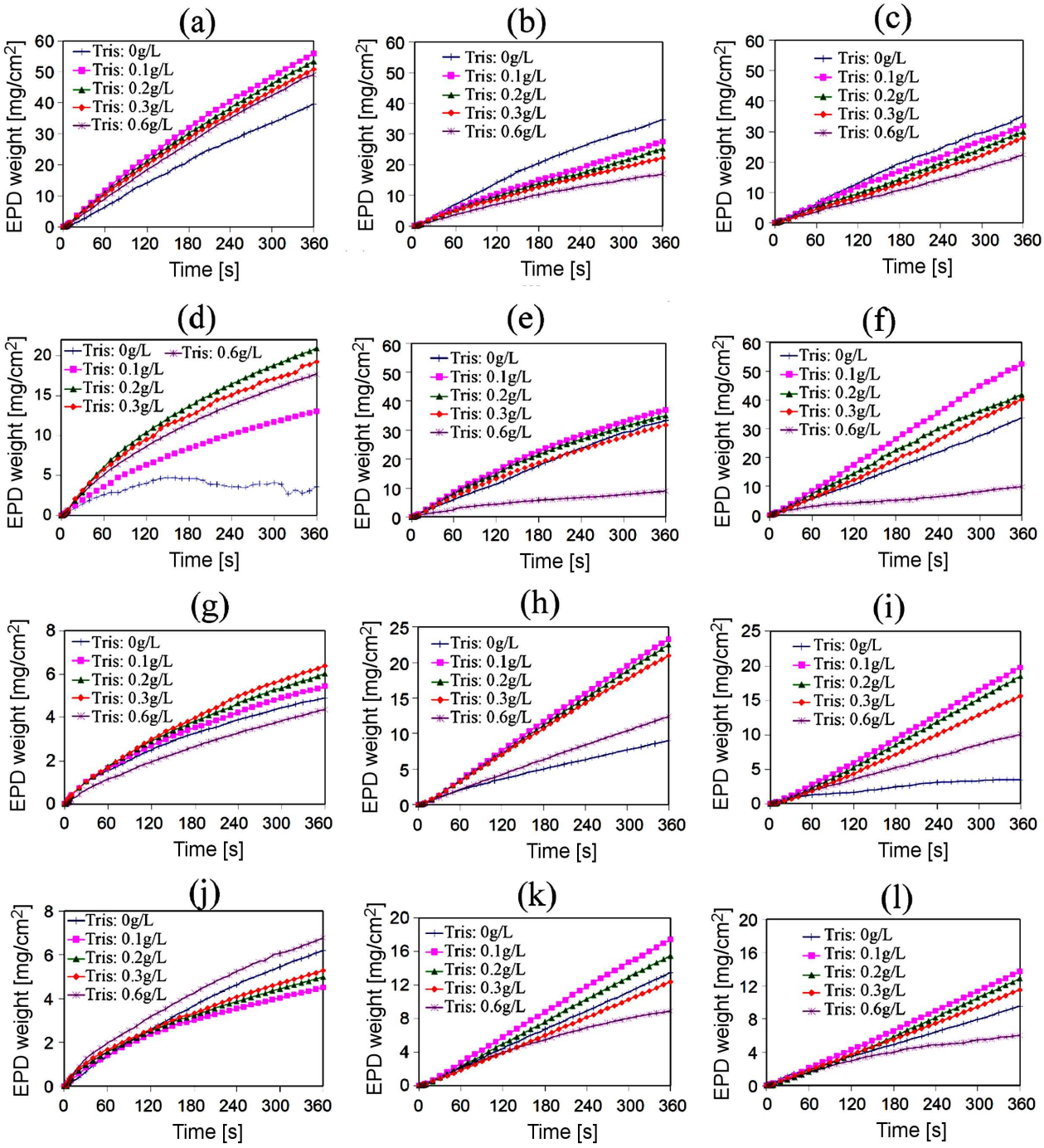

Figure 6. ***In-situ*** **kinetics of EPD at 60 V (for methanolic suspensions: 20 V) from different alcoholic suspensions of titania nanoparticles (20 g/l) ((a-c): methanolic, (d-f): ethanolic, (g-i): isopropanolic and (j-l): butanolic) with various concentrations of Tris and AA ((a-j): 0, (b-k): 0.2 and (c-l): 0.53 vol.%)**

coating deposited from the Tris-free suspension must be sintered at more elevated temperatures which can result in its better consolidation.

The SEM images of the sintered coating before and after its immersion in SBF solution for 1 week are shown in Figs. 8a and 8b, respectively. The EDXS spectrum of the coating after its immersion in the SBF is also shown in Fig. 8c. As it can be seen, the microstructure of the sintered coating (Fig. 8a) is slightly coarser and more compact than that of green coating (Fig. 6b). However, the sintering temperature used in this work is not high enough to completely consolidate the coating. High sintering temperatures lead to the annealing of metallic substrate and considerable drop in its mechanical properties. On the other hand, the open microstructure of bioactive coatings accelerates implant fixation by bone ingrowths into their pores. As it can be seen the surface of the titania coating is completely covered by the layer with worm-like morphology typical of hydroxyapatite (HA) after one week of immersion in SBF.

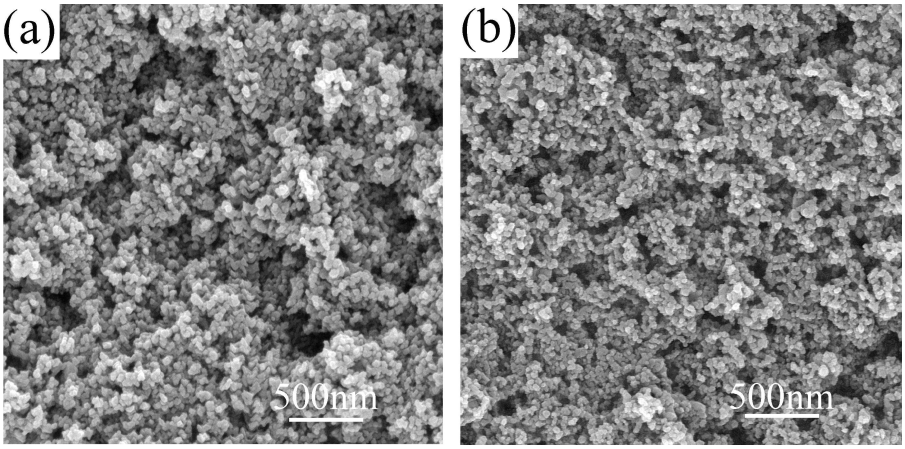

Figure 7. SEM images for the dried coating deposited at 20 V for 30 s from the methanolic suspension without (a) and with (b) 0.1 g/l Tris

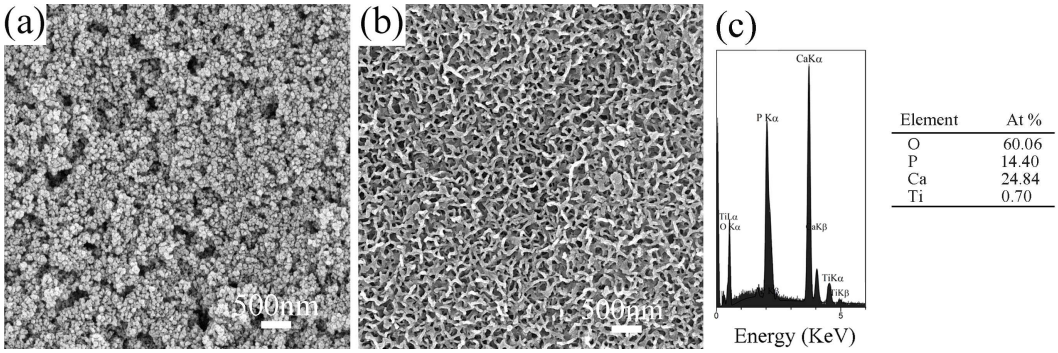

Figure 8. SEM image of the sintered coating deposited at 20 V for 30 s from the methanolic suspension with 0.1 g/l Tris before (a) and after (b) the immersion in SBF for one week, and EDXS analysis from the coating after immersion in SBF for one week (c)

The EDXS analysis prove that this layer is mainly composed of oxygen, calcium and phosphor; the spectra also show the negligible amount of titanium in the composition of the layer originating from the underlay titania coating. The EDS results show that ratio of Ca/P is 1.725 for generated layer slightly less than that of pure HA (Ca/P = 1.67). The higher Ca/P ratio can be due to the formation of carbonated HA in which some $(PO_4)_3^-$ groups of HA are replaced by $(CO_3)^{2-}$ groups. So HA are formed on the surface of titania coating after its immersion for one week in SBF environment showing its good bioactivity.

Figure 9 shows the Nyquist curves for bare substrate and the one coated with optimum coating. As it can be seen the impedance of coated substrate is considerably higher than that of uncoated one implying that the optimum coating can prevent from implant corrosion in SBF by acting as the effective barrier against corrosive medium preventing from its reaching to the metallic surface of implant.

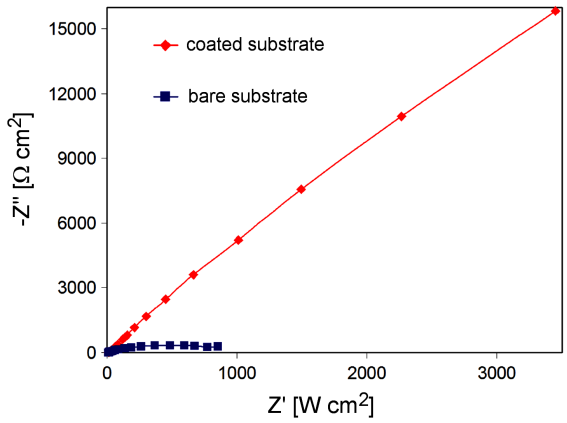

Figure 9. Nyquist curves for bare substrate and the one coated with optimum coating in SBF environment at 37.5 °C

IV. Conclusions

Tris was used as the dispersant to stabilize titania nanoparticles in different alcoholic suspensions. It was found that Tris molecules are protonated in alcoholic suspensions to generate H^+Tris ions. The generated H^+Tris ions are then adsorbed on the particles and enhance their surface charge. Also the optimum concentration of Tris increased with molecular size of alcohol (0.1, 0.2, 0.3 and 0.6 g/l in methanolic, ethanolic, isopropanolic and butanolic suspensions, respectively). Acetic acid (AA) was added into the suspensions to promote the ionization of Tris. The zeta potential of particles continuously decreased with Tris addition into AA containing methanolic suspensions. However, for other alcoholic suspensions with AA, the optimum concentra-

tion of Tris was shifted to lower amount of Tris (0.1 g/l). The kinetics of EPD was the fastest from the suspensions with the optimum concentration of Tris (the highest zeta potential). Calcium phosphate compounds with worm-like morphology were formed on the surface of titania coating after its immersion for one week in SBF at 37.5 °C.

References

1. R.J. Isaifan, A. Samara, W. Suwaileh, D. Johnson, W. Yiming, A.A. Abdallah, B. Aïssa, "Improved self-cleaning properties of an efficient and easy to scale up TiO_2 thin films prepared by adsorptive self-assembly", *Sci. Reports*, **7** (2017) 9466.
2. L. Bergamonti, G. Predieri, Y. Paz, L. Fornasini, P.P. Lottici, F. Bondioli, "Enhanced self-cleaning properties of N-doped TiO_2 coating for cultural heritage", *Microchem. J.*, **133** (2017) 1–12.
3. J. Esparza, G.G. Fuentes, R. Bueno, R. Rodríguez, J.A. García, A.I. Vitas, V. Rico, A.R. Gonzalez-Elipe, "Antibacterial response of titanium oxide coatings doped by nitrogen plasma immersion ion implantation", *Surf. Coating Technol.*, **314** (2017) 67–71.
4. N.S. Leyland, J. Podporska-Carroll, J. Browne, S.J. Hinder, B. Quilty, S.C. Pillai, "Highly efficient F, Cu doped TiO_2 anti-bacterial visible light active photocatalytic coatings to combat hospital-acquired infections", *Sci. Reports*, **6** (2016) 24770.
5. S. Atefyekta, B. Ercan, J. Karlsson, E. Taylor, S. Chung , T.J. Webster, M. Andersson, "Antimicrobial performance of mesoporous titania thin films: role of pore size, hydrophobicity, and antibiotic release", *Int. J. Nanomed.*, **11** (2016) 977–990.
6. M. Aflori, B. Simionescu, I.E. Bordianu, L. Sacarescu, C.D. Varganici, F. Doroftei, A. Nicolescu, M. Olaru, "Silsesquioxane-based hybrid nanocomposites with methacrylate units containing titania and/or silver nanoparticles as antibacterial/antifungal coatings for monumental stones", *Mater. Sci. Eng. B*, **178** (2013) 1339–1346.
7. A.V. Baglov, N.M. Denisov, V.E. Borisenko, V.V. Uglov, A.A. Malashevich, "Photocatalytic activity of nanostructured titania coatings on aluminum substrates", *Inorgan. Mater.*, **53** (2017) 1180–1184.
8. X. Wang, R. Yu, K. Wang, G. Yang, H. Yu, "Facile template-induced synthesis of Ag-modified TiO_2 hollow octahedra with high photocatalytic activity", *Chin. J. Catal.*, **36** (2015) 1211–2218.
9. R. Quesada-Cabrera, A. Mills, Ch. O'Rourke, "Action spectra of P25 TiO_2 and a visible light absorbing, carbon-modified titania in the photocatalytic degradation of stearic acid", *Appl. Catal. B*, **150-151** (2014) 338–344.
10. X. Rao, J. Li, X. Feng, C. Chu, "Bone-like apatite growth on controllable macroporous titanium scaffolds coated with microporous titania", *J. Mech. Behav. Biomed. Mater.*, **77** (2018) 225–233.
11. A. Gao, R. Hang, X. Huang, L. Zhao, X. Zhang, L. Wang, B. Tang, S. Ma, P.K. Chu, "The effects of titania nanotubes with embedded silver oxide nanoparticles on bacteria and osteoblasts", *Biomaterials*, **35** (2014) 4223–4235.
12. A. Calia, M. Lettieri, M. Masieri, S. Pal, A. Licciulli, A. Arima, "Limestones coated with photocatalytic TiO_2 to enhance building surface with self-cleaning and depolluting abilities", *J. Clean. Prod.*, **165** (2017) 1036–1047.
13. M. Wilson, C.Y.C. Cheng, G. Oswald, R. Srivastava, S.K. Beaumont, J.P.S. Badyal, "Magnetic recyclable microcomposite silica-steel core with TiO_2 nanocomposite shell photocatalysts for sustainable water purification", *Colloids Surf. A*, **523** (2017) 27–37.
14. G. Plesch, M. Vargová, U.F. Vogt, M. Gorbár, K. Jesenák, "Zr doped anatase supported reticulated ceramic foams for photocatalytic water purification", *Mater. Res. Bull.*, **47** (2012) 1680–1686.
15. J.M. Calderon-Moreno, "Effect of polyethylene glycol on porous transparent TiO_2 films prepared by sol-gel method", *Ceram. Int.*, **40** (2014) 2209–2220.
16. L. Ćurković, H. Otmačić Ćurković, S. Salopek, M. Majić Renjo, S. Šegota, "Enhancement of corrosion protection of AISI 304 stainless steel by nanostructured sol-gel TiO_2 films", *Corrosion Sci.*, **77** (2013) 176–184.
17. M.B. Zakaria, M.A, Elmorsi, E.Z.M. Elbeid, "Nanostructured žce coated stainless steel for corrosion protection", *J. Nanosci. Nanotechnol.*, **16** (2016) 9215–9222.
18. Y. Ando, D. Kindole, Y. Noda, R.N. Mbiu, B.K. Kosgey, S.M. Maranga, A. Kobayashi, "Alumina and titania films deposition by APS/ASPPS dual mode thermal spray equipment using Ar added N_2 working gas", *Vacuum*, **136** (2017) 203–207.
19. K. Ren, Y. Liu, X. He, H. Li, "Suspension plasma spray fabrication of nanocrystalline titania hollow microspheres for photocatalytic applications", *J. Therm. Spray Tech.*, **24** (2015) 1213–1220.
20. J. Gao, Ch. Zhao, J. Zhou, Ch. Li, Y. Shao, Ch. Shi, Y. Zhu, "Plasma sprayed rutile titania-nanosilver antibacterial coatings", *Appl. Surf. Sci.*, **355** (2015) 593–601.
21. D. Wei, Y. Zhou, D. Jia, Y. Wang, "Chemical treatment of TiO_2-based coatings formed by plasma electrolytic oxidation in electrolyte containing nano-HA, calcium salts and phosphates for biomedical applications", *Appl. Surf. Sci.*, **254** (2008) 1775–1782.
22. B. Scheffel, T. Modes, C. Metzner, "Reactive high-rate deposition of titanium oxide coatings using electron beam evaporation, spotless arc and dual crucible", *Surf. Coating Technol.*, **287** (2016) 138–144.
23. W. Zhao, X. Feng, X. Ma, L. He, Q. Cao, J. Ma, "Structural and optical properties of heteroepitaxial anatase titania films on $MgAl_6O_{10}$ (100) substrates by MOCVD", *Appl. Surf. Sci.*, **426** (2017) 369–375.
24. L. Ren, Y.P. Zeng, D. Jiang, "Preparation of porous TiO_2 sheets by aqueous tape casting and their photocatalytic activation", *Int. J. App. Ceram. Technol.*, **5** (2008) 505–512.
25. L. Besra, M. Liu, "A review on fundamental and applications of electrophoretic deposition", *Prog. Mater. Sci.*, **52** (2007) 1–61.
26. T. Uchikoshi, K. Ozawa, B.D. Hatton, Y. Sakka, "Electrophoretic deposition of alumina suspension in a strong magnetic field", *J. Mater. Res.*, **16** (2001) 321–324.
27. M. Farrokhi-Rad, M. Ghorbani, "Electrophoretic deposition of titania nanoparticles in different alcohols: kinetics of deposition", *J. Am. Ceram. Soc.*, **94** (2011) 2354–61.
28. M. Farrokhi-Rad, "Electrophoretic deposition of hydroxyapatite nanoparticles in different alcohols: Effect of Tris (tris(hydroxymethyl)aminomethane) as a dispersant", *Ceram. Int.*, **42** (2016) 3361–3371.
29. M. Farrokhi-Rad, T. Shahrabi, F. Shahriari, "Elec-

trophoretic deposition of titania-carbon nanotubes nanocomposite coatings in different alcohols", *J. Eur. Ceram. Soc.*, **34** (2014) 4411–4424.
30. M. Farrokhi-Rad, T. Shahrabi, "Effect of suspension medium on the electrophoretic deposition of hydroxyapatite nanoparticles and properties of obtained coatings", *Ceram. Int.*, **40** (2014) 3031–3039.
31. M. Farrokhi-Rad, T. Shahrabi, "Electrophoretic deposition of titania nanoparticles: sticking parameter determination by an in situ study of the EPD kinetics", *J. Am. Ceram. Soc.*, **95** (2012) 3434–3440.
32. T. Kokubo, H. Takadama, "How useful is SBF in predicting in vivo bone bioactivity?", *Biomaterials*, **27** (2006) 2907–2915.
33. S.G.J. Heijman, H.N. Stein, "Electrostatic and sterical stabilization of TiO_2 dispersions", *Langmuir*, **11** (1995) 422–427.
34. J.B. Paul, R.A. Provencal, C. Chapo, K. Roth, R. Casaes, R.J. Sakally, "Infrared cavity ringdown spectroscopy of the water cluster bending vibrations", *J. Phys. Chem. A*, **103** (1999) 2972–2974.
35. Y. Shen, P. Wu, "Two-dimensional ATR-FTIR spectroscopic investigation on water diffusion in polypropylene film: Water bending vibration", *J. Phys. Chem. A*, **107** (2003) 4224–4226.
36. D.L. Pavia, G.M. Lampman, G.S. Kriz, James A. Vyvyan, "Infrared spectroscopy", pp. 15–104 in *Introduction to Spectroscopy*, Eds. by L. Lockwood, B. Kirksey, E. Woods, K. Brown, B. Kauser. Thomson Learning Inc, New York, USA, 2001.
37. R.N. Basu, C.A. Randall, M.J. Mayo, "Fabrication of dense zirconia electrolyte films for tubular solid oxide fuel cells by electrophoretic deposition", *J. Am. Ceram. Soc.*, **84** (2001) 33–40.